# CALCULATION OF TRANSIENT COMBUSTION REGIMES FOR SOLID PROPELLANT IN A CHANNEL

V. B. Librovich and G. M. Makhviladze

In the study of solid-propellant transient-burning processes the case of solids containing an oxidizer in their composition was examined in [1-8]. The theory of unsteady combustion processes of such propellants was given in [1-3]. A numerical calculation was made in [4] of the transient processes from the steady-state burning regime at one pressure to the steady-state regime at a different pressure, using an electronic computer. In [5] the method of integral relations was used to derive analytic expressions for the unsteady solid burning rate for instantaneous and exponential variation of the pressure. The effect on solid propellant burning velocity of harmonically varying pressure was studied in [6]. The unsteady processes in the burning of solid propellants were investigated in [7].

In the following we examine the transient regimes for diffusive combustion, which occurs when the oxidizer is supplied from outside and does not form part of the solid propellant. The transition from one burning regime to another is specified by variation of the oxidizer flowrate. Combustion models for such systems were proposed in [9, 10]. In calculating the transient regimes we use the combustion model based on the limiting role of mass transfer in diffusive combustion [10]. In view of the finite time for emptying of the propellant channel through the nozzle (with reduction of the oxidizer flowrate) or filling of the channel (with increase of the oxidizer flowrate), the pressure in the channel will lag behind the change in oxidizer flowrate. Moreover, the transient regimes are characterized by formation in the channel of gasdynamic waves which cause pressure pulsations as they are reflected alternately from the head and nozzle ends of the channel. The solid propellant combustion velocity depends on the mass velocity of the gas stream; therefore channel burnup takes place nonuniformly. A system of equations describing the steady-state and transient combustion regimes and a finite-difference scheme for the integration of this system are proposed. The behavior pattern of the solutions obtained are discussed.

## PROBLEM FORMULATION

Let the fuel have the form of a cylindrical grain with axial channel of radius R, through which the oxidizer stream flows. We direct the x axis along the axis of symmetry; $x = 0$ coincides with the beginning of the channel. The channel length is $l$. The channel is throttled by a supersonic nozzle. We shall solve the problem under the following assumptions.

1°. The flow is one-dimensional and turbulent along the entire channel length. We neglect the nonuniformity of the flow in the transverse y and z directions, which can occur as a result of expansion or curvature of the channel walls, efflux from the walls of the combustion products, as a result of friction or heat transfer. The naturalness of this assumption is confirmed by the fact that the gas motion in the channel is turbulent and the turbulence is intensified by heat and mass addition as a result of the chemical combustion reaction taking place at the walls (see 2°). We note that the one-dimensional model presumes complete mixing of the oxidizer and combustion products at each section of the channel.

2°. In the channel diffusive combustion takes place at the walls (this model was discussed in [10]), i.e., above the surface of the fuel there develops a diffusion flame of chemical reaction of the solid fuel gasification products with the gaseous oxidizer flowing past the fuel surface, and this flame is located in the boundary layer. We note that the distance from the flame to the fuel surface is inversely proportional

Moscow. Translated from Zhurnal Prikladnoi Mekhaniki i Tekhnicheskoi Fiziki, Vol. 10, No. 5, pp. 33-41, September October, 1969. Original article submitted April 16, 1969.

to the burning velocity [10]. Therefore the assumption made here is valid as long as the oxidizer concentration in the flow is not too small. In fact, as the oxidizer concentration diminishes (i.e., with increase of x) the diffusion flame moves away from the surface of the solid fuel; therefore the fuel flame is increasingly subject to the action of the outer turbulent flow. As a result the flame is deformed and becomes ragged, discontinuities may appear on the flame surface; then a qualitatively different mechanism for breakdown of the solid fuel begins to play a role – namely, ablation. Therefore we shall assume that the channel is not too long and the Reynolds numbers, which determine the burning velocity, are not very large. Since the flame is located in the depth of the boundary layer we shall assume that the chemical reaction is concentrated at the channel walls.

3°. The gas is assumed to be ideal and of constant molecular weight.

4°. We also neglect the change of the channel shape and dimensions in the course of the transient process.

5°. We neglect the dependence of the thermal effect on the gas flow parameters, i.e., we assume that the heated fuel layer adjusts instantaneously to the state of the gas flow.

6°. The gas motion is turbulent, therefore it is natural to neglect the molecular transport phenomena as well.

Equations and Boundary Conditions. Before writing out the system of equations we note that the solid fuel burning velocity can be written in the form

$$m = B_m a j^n \tag{2.1}$$

Here m is the mass burning velocity of the solid fuel, $a$ is the relative weight concentration of the oxidizer, $B_m$ and n are constants, and j is the mass velocity of the gas flow.

Expression (2.1) for the burning velocity can be obtained by using the condition for the stoichiometric relation between the fuel and oxidizer flows in the diffusion flame and calculating the mass transfer coefficient from the criterial connection between the diffusive Nusselt number, the Reynolds and Prandtl numbers, and the ratio of the gas efflux velocity from the fuel to the longitudinal velocity of the oxidizer stream [10].

We shall use as the governing equations the one-dimensional gasdynamic equations with account for the heat and mass sources concentrated at the walls. In view of the fact that in calculating the transient regimes the magnitude of the gas flowrate, the gas concentration, and also the enthalpy will be specified at the entrance to the channel, it is convenient to write the system of equations in terms of the dependent variables j, p (gas pressure), $a$, H (gas enthalpy), using the expression (2.1) for m.

We introduce dimensionless variables (denoted by primes)

$$j' = \frac{j}{j_0}, \quad H' = \frac{H}{H_0}, \quad a' = \frac{a}{a_0}, \quad x' = \frac{x}{l}, \quad p' = \frac{p}{j_0\sqrt{H_0}}, \quad t' = \frac{t\sqrt{H_0}}{l}, \quad Q' = \frac{Q}{H_0} \tag{2.2}$$

The subscript 0 denotes the value of the given quantity at the section x = 0, Q is the effective burning thermal effect per unit weight of the solid fuel, t is time.

In these variables (we drop the primes hereafter) the system of equations has the form

$$\frac{\partial w}{\partial t} + \frac{\partial f}{\partial x} = s \tag{2.3}$$

Here w, $f$, s are single-column matrices with the components

$$w_1 = \frac{\gamma p}{(\gamma-1)H}, \quad w_2 = \frac{\gamma p a}{(\gamma-1)H}, \quad w_3 = j, \quad w_4 = \frac{p}{\gamma-1} + \frac{1}{2}\frac{\gamma-1}{\gamma}\frac{j^2H}{p}$$

$$f_1 = j, \quad f_2 = aj, \quad f_3 = p + \frac{\gamma-1}{\gamma}\frac{j^2H}{p}, \quad f_4 = jH + \frac{1}{2}j\left(\frac{\gamma-1}{\gamma}j\frac{H}{p}\right)^2 \tag{2.4}$$

$$s_1 = \nu_1 K a j^n, \quad s_2 = -\frac{\nu_2}{a_0}Kaj^n, \quad s_3 = 0, \quad s_4 = QKaj^n \left(K = 2\frac{l}{R}B_m a_0 j_0^{n-1}\right)$$

Here $\gamma$ is the adiabatic exponent of the gas, $\nu_1 = (\nu_2 + 1)$ is the stoichiometric coefficient.

To solve this system we pose the three boundary conditions at the channel entrance

$$x = 0, \quad j = h(t), \quad a = 1, \quad H = 1 \tag{2.5}$$

The function h(t) specifies the transition from one burning regime to another. Assume that a constant oxidizer flowrate equal to $a_0 j_0 \pi R^2$ was maintained at the channel entrance for $t < 0$. As a result the steady-state burning regime corresponding to this oxidizer flowrate was established. The corresponding steady-state solution, found below, will serve as the initial condition for the solution of the unsteady system of equations (2.3). Then, beginning at the time t = 0 there is a sharp change of the oxidizer flowrate by several fold, specified by the function h(t), which causes transition to another steady-state burning regime corresponding to the new oxidizer flowrate.

The fourth boundary condition accounts for the presence of the Laval nozzle. If we assume that the gas flow through the nozzle is quasisteady, adjusting to the state of the gas at the entrance to the nozzle, we can use the known expression

$$j_l R^2 = A p_l R_*^2 \qquad \left(A = \sqrt{\gamma}\left(\frac{2}{\gamma+1}\right)^{1/2\alpha}(R^0 T_l)^{-1/2}, \quad \alpha = \frac{\gamma+1}{\gamma-1}\right) \tag{2.6}$$

Here A is the coefficient of gas discharge through the nozzle, $R^0$ is the gas constant, T is the temperature in the gas stream, R* is the radius of the nozzle throat, the subscript $l$ indicates the value of the given quantity at the section $x = l$. Separating the temperature dependence in (2.6) and converting to dimensionless variables, we have

$$x = 1, \quad p_l = \frac{1}{\varkappa} j_l H_l^{1/2} \qquad \left(\varkappa = \frac{\gamma}{(\gamma-1)^{1/2}}\left(\frac{2}{\gamma+1}\right)^{1/2\alpha}\left(\frac{R_*}{R}\right)^2\right) \tag{2.7}$$

Solution of the Steady-State Problem of Burning in a Fuel Channel. Let us find the steady-state solution of (2.3) with the boundary conditions (2.5), (2.7). (In this case $h(t) \equiv 1$.) Dropping the derivatives with respect to t in (2.3) and combining the last three equations with the first, we obtain the dependence of p, H, $a$ on j, $p_0$ and the boundary conditions for x = 0

$$\begin{aligned} a &= \frac{1}{j}\left[1 - \frac{\nu_2}{\nu_1 a_0}(j-1)\right], \quad H = \frac{\gamma p}{(\gamma-1)j^2}(\beta - p) \quad \left(\beta = p_0 + \frac{\gamma-1}{\gamma p_0}\right) \\ p &= \frac{1}{\gamma+1}\left\{\beta + \left\{\gamma^2\beta^2 + 2(\gamma^2-1)\, j\left[\frac{Q}{\nu_1}(1-j) - 1 - \frac{1}{2}(\beta - p_0)^2\right]\right\}^{1/2}\right\} \end{aligned} \tag{3.1}$$

Substituting the expression for $a$ into the first steady-state equation (2.3), we obtain the differential equation describing the variation of the gas stream along the channel axis

$$\frac{dj}{dx} = \nu_1 K j^{n-1}\left(1 - \frac{\nu_2(j-1)}{\nu_1 a_0}\right) \tag{3.2}$$

For arbitrary values this expression can only be integrated numerically,* however we can obtain analytic expressions for n = 0.5 and n = 1.0 which majorize from below and from above the real relation j = j(x) for $0.5 < n < 1$. We present these relations

$$j = 1 + \frac{\nu_1 a_0}{\nu_2}\left[1 - \exp\left(-\frac{\nu_2}{a_0} Kx\right)\right] \qquad (n = 1)$$

$$2(d^2-1)\left[1 - \sqrt{j} + \frac{d}{2}\ln\frac{(d+\sqrt{j})(d-1)}{(d-\sqrt{j})(d+1)}\right] = \nu_1 Kx \qquad (n = 0.5) \tag{3.3}$$

$$d = \left(1 + \frac{\nu_1 a_0}{\nu_2}\right)^{1/2} \tag{3.4}$$

*The Euler method was used for the numerical computation. The interval of values from 0 to 1 was divided into 100 parts, so that $x_i = i\Delta x$, where $\Delta x = 0.01$, $i = 0, 1, 2, \ldots, 100$. The finite-difference equation corresponding to the differential equation (3.2) has the form

$$j(x_i + \Delta x) = j(x_i) + \Delta x\left(\nu_1 + \frac{\nu_2}{a_0}\right) K[j(x_i)]^{n-1} - \Delta x \frac{\nu_2}{a_0} K[j(x_i)]^n$$

This equation makes it possible to calculate the flux j for all x. The results of the calculations are shown in Fig. 1. Curve 3 was obtained by numerical calculation for n = 0.76; curves 6 and 7 were plotted for n = 1 and n = 0.5 (remaining parameters are the same). We see from the figure that the steady-state solution can be obtained from the analytic expressions (3.3), (3.4) with good accuracy.

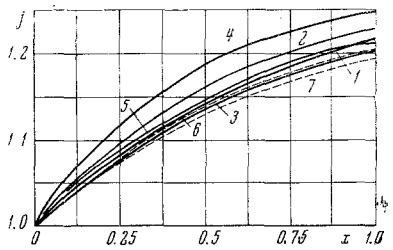

Fig. 1

We can determine the quantity $j_l$ from (3.2). Writing the second and third equations (3.1) for $x = l$ and using the boundary condition (2.7), we obtain a system of equations from which we find the dependence of the channel entrance pressure $p_0$ on $j_l$

$$p_0^2 = \frac{\gamma-1}{\gamma\varepsilon}\left[\sigma - \varepsilon + \left(\sigma^2 - 2\sigma\varepsilon + \frac{\gamma-1}{\gamma}\varepsilon\right)^{1/2}\right]$$
$$\sigma = 1 + \frac{Q}{\nu_1}(j_l - 1), \quad \varepsilon = \varkappa^2\frac{\gamma-1}{\gamma l}\left[2 + \left(\frac{\gamma-1}{\gamma}\varkappa\right)^2\right]\left(1 + \frac{\gamma-1}{\gamma}\varkappa^2\right)^{-2} \qquad (3.5)$$

Now all the other functions are found easily from (3.1).

In the calculation we used various values of the dimensionless parameters appearing in the equations and the boundary conditions.

1°. We set $\gamma = 1.276$, $\varkappa = 0.3182$, $Q = 33.33$, $a_0 = 0.22$, $n = 0.76$, $\nu_1 = 4.43$. With these values the calculation was made for $K_1 = 0.0906$, $K_2 = 0.0822$, $K_3 = 0.1070$.

The parameter $K_1$ corresponds to twice the oxidizer flowrate at the channel entrance as for the parameter $K_3$ and the parameter $K_2$ corresponds to a flowrate 1.5 times that of $K_1$ (other parameters remaining the same).

The resulting steady-state solutions are shown in Fig. 1 and are denoted by 1, 2, 3 in accordance with the number K. The point $x = 1.0$ on the abscissa axis corresponds to the end of the channel.

We note that the flow at the end of the channel increases by 21.3% for case 1. The amount of oxidizer carried away together with the gas stream through the nozzle amounts to 20.7% of the amount of oxidizer entering the channel. From the third equation (2.3) we have

$$p_l = p_0\,(1 + \gamma M_0^2)\,/\,(1 + \gamma M_l^2) \qquad (3.6)$$

where M is the Mach number. Since the motion in the channel is essentially subsonic ($M_0 = 0.08$, $M_l = 0.13$ for case 1), the pressure decreases only slightly along the channel axis: $p_0 = 5.66$ and decreases by 1.5% toward the end of the channel.

In this case the gas enthalpy increases by 114% at the channel exit section. Thus the relative mass flow increase is considerably less than the relative gas enthalpy increase.

In conclusion, we present the values of the time for gas passage through the channel (or the time for emptying the fuel channel) $t_1 = 12.5$ and the time for the propagation of a sound disturbance $t_2 = 1.4$ (these characteristic times are approximately the same for all three cases).

2°. We set $\gamma = 1.283$, $\varkappa = 0.5141$, $Q = 36.50$, $a_0 = 0.21$, $n = 0.76$, $\nu_1 = 4.43$. With these parameters the calculation was made for $K_4 = 0.1447$ and $K_5 = 0.0935$.

The parameter $K_5$ corresponds to 6.17 times more oxidizer flowrate through the channel than for $K_4$ (other parameters remaining the same).

The solutions for these two cases are shown in Fig. 1 and denoted by numerals 4 and 5 in accordance with the number K. The behavior of the solutions is the same as in case 1°. In this case $t_1 = 7.1$, $t_2 = 1.2$.

Integration of the Unsteady Equations. The unsteady problem was solved numerically using the two-layer explicit difference scheme of second-order accuracy proposed in [11]. The artificial viscosity (required for automatic calculation of the shocks) appears implicitly in (4.1) as a result of approximation of the differential equations by finite-difference equations. All the quantities are taken at the grid nodes $x_i = i\Delta x$, $i = 0, \ldots, 100$; $t = m\Delta t$, $m = 0.1 \ldots$ We write out this scheme

$$w_{i+1/2}\left(t + \frac{\Delta t}{2}\right) = \frac{w_{i+1}(t) + w_i(t)}{2} - \frac{\Delta t}{2\Delta x}\left[f_{i+1}(t) - f_i(t)\right] + \frac{\Delta t}{2}s_{i+1/2}(t)$$
$$w_i(t + \Delta t) = w_i(t) - (\Delta t/\Delta x)\left[f_{i+1/2}(t + 1/2\,\Delta t) - f_{i-1/2}(t + 1/2\,\Delta t)\right] + \Delta t s_i(t + 1/2\,\Delta t) \qquad (4.1)$$

All the quantities are first calculated on the half-integral layer at the time $t + 1/2\,\Delta t$ from the first-order accuracy scheme (first equation (4.1) and then at the time $t + \Delta t$ using the quantities on the half-integral layer, so that as a result the scheme (4.1) has second-order accuracy.

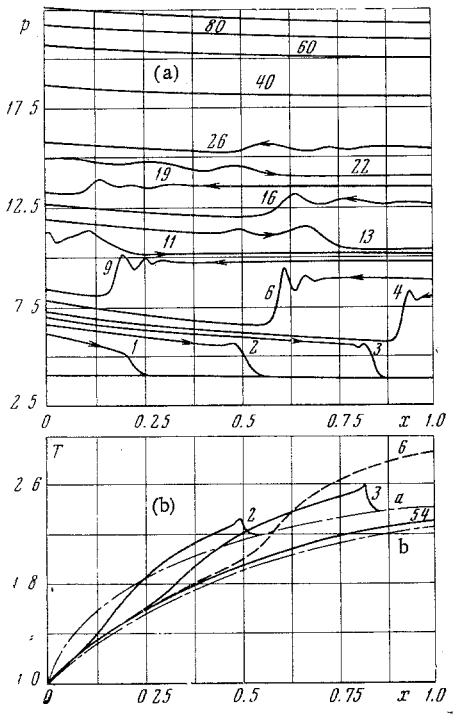


Fig. 2

To improve the computational efficiency, in place of the sharp change (step) in the oxidizer flowrate we used a smooth (exponential) transition to the new flowrate, i.e.,

$$h(t) = k + (1 - k)\, e^{-\lambda m \Delta t} \qquad (4.2)$$

Here k is the final gas flowrate at the channel entrance (initial value was 1) in the transient regime; $\lambda$ was selected so that the new oxidizer flowrate was established quite rapidly. The calculations were made for three cases. The transients were investigated for k = 6.17, 0.5, 1.5.

In order for the selected difference scheme to be stable (i.e., in order that small errors which arise in the computational process not grow), the relationship between the time and coordinate steps must satisfy the Courant – Friedrichs – Levy stability criterion, namely

$$\max_x (|u| + c)\, \Delta t/\Delta x \leqslant 1$$

The step in x was selected as in the steady case ($\Delta x = 0.01$ in dimensionless form), the gas velocity u and the sound speed c were estimated from the steady temperature profile, after which the quantity $\Delta t$ was calculated. Points on the boundary were refined using a five point scheme. The computation was terminated when the distributions of all the quantities became close to their final steady state distributions.

## DISCUSSION OF RESULTS

1°. Let us first examine how the transient takes place for k = 6.17, i.e., from the steady regime corresponding to $K_4 = 0.1447$ to the new steady regime corresponding to $K_5 = 0.0935$ (the other numerical parameters are the same as in 2° of Section 3).

In Fig. 2a and b the abscissa is the distance from the channel entrance to the beginning of the nozzle, and the point x = 1.0 corresponds to the end of the channel. The ordinate is the dimensionless pressure (Fig. 2a) and temperature (Fig. 2b). The coordinate step $\Delta x = 0.01$; the time step $\Delta t = 0.0075$. The solutions are shown at different moments of time. The time scale $\Delta T = 0.3075$, i.e., the curve denoted by the numeral 3 is the solution at the moment $3\Delta T$ (some intermediate curves are not shown to avoid confusion in the figure).

The upper curve in Fig. 2a is the final steady pressure profile ($K = K_5$), the lower curve is the initial steady pressure profile ($K = K_4$). The time for establishing the new oxidizer flowrate at the channel entrance is $\Delta T$.

We see from the figure that after change of the oxidizer flowrate a shock wave begins to propagate through the channel (in all the figures the direction of propagation of the shock wave is indicated by the arrow), which after reaching the nozzle is reflected from the nozzle and begins to propagate in the opposite direction; then it is reflected from the left boundary and so on. The initial wave intensity is $\Delta p/p_1 = 0.4$, (ratio of the pressure differential across the wave front to the pressure in the undisturbed region). There is a dip in curve 2. This indicates the appearance of a rarefaction wave, which develops as a result of decay of the developing discontinuity.

Figure 2b (see curves 2,3) shows that heating of the gas by the shock wave is quite significant. Let us make an estimate of the gas temperature rise in the wave front at the moment $3\Delta T$. Knowing $\Delta p/p_1$, we find from the Rankine – Hugoniot relations that the ratio of the gas temperature behind the shock wave to the temperature in the undisturbed region is 1.08. This agrees with the ratio of these temperatures calculated for curve 3 from Fig. 2b. We note that the gas temperature at the exit from the channel in the initial steady state is higher than the gas temperature in the final steady state by a factor of 1.07 (the curves labeled a and b are the initial and final steady-state distributions); however, as a result of heating of the gas by the shock wave its temperature may be higher than the initial value. Upon reflection of the

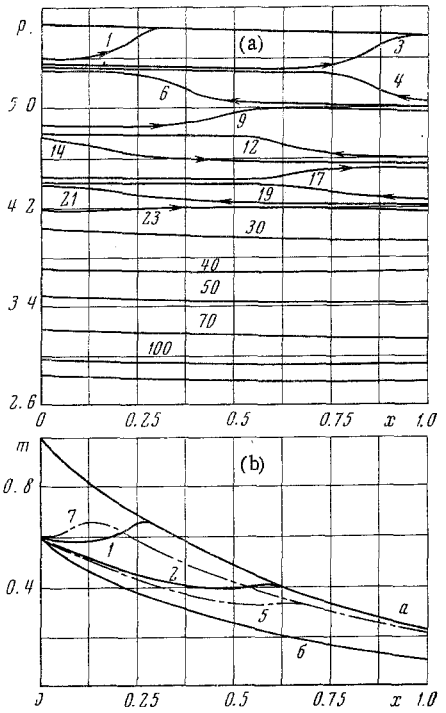

Fig. 3

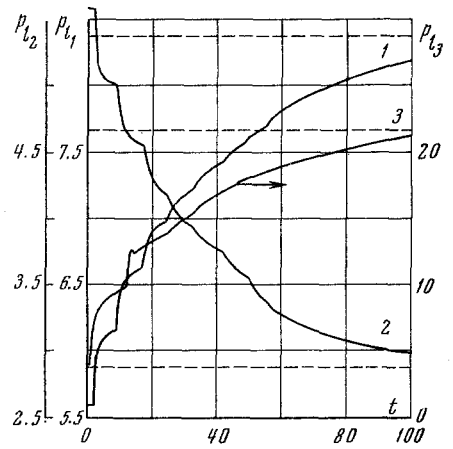

Fig. 4

wave from the nozzle (Fig. 2a, curve 6) a high-temperature gas slug is formed (Fig. 2b, curve 6). Then this slug begins to slowly dissipate, since the gas discharges through the nozzle. The temperature gradually decreases to the steady-state value corresponding to $K = K_5$ (Fig. 2b, curve 54).

The shock wave propagates toward the left boundary with a velocity approximately half (relative to the channel walls) that of the wave propagating toward the nozzle. This is explained by the fact that the wave is traveling in the direction opposite the direction of the gas flow. The shock wave velocity relative to the walls is twice that of sound (estimated using curves 2 and 3 in Fig. 2a).

The reflection of the shock wave from the boundaries takes place like reflection from solid walls. This is explained by the fact that the gas velocity in the channel is low; therefore during the time of wave reflection from the boundary only a very small part of the wave can pass into the nozzle.

During shock wave reflection from the nozzle a small second hump forms on its profile, which is apparently associated with the formation of a rarefaction wave during reflection from the nozzle.

The shock wave decay, which is seen in Fig. 2a, takes place primarily in the volume. Decay of the wave is accompanied by diffusion of its front. Reduction of the wave intensity takes place because:

a) part of the gas does manage to pass into the nozzle during the reflection time;

b) there is interaction of the compression wave with the rarefaction waves;

c) the wave propagates through a nonhomogeneous medium (specifically, after reflecting from the nozzle the wave travels through gas whose pressure increases with decrease of x).

We see from Fig. 2a that the wave decay in this case is very marked during its interaction with the gas entering the channel (curves 6 and 9), i.e., for the third reason. The times for wave decay (here we have in mind the time for marked reduction of the wave intensity) and for transition to the new steady-state regime will be presented below.

After decay of the shock wave there is a smooth pressure rise up to the final steady-state distribution because of propagation through the channel of compression waves of low intensity (therefore they are not noticeable in the figure). In addition to the gradually decaying wave which develops at the initial moment, these waves are generated at the point where the gas entering the channel at the moment $t = 0$ compresses the gas being displaced.

2°. Figure 3a shows the pressure distribution along x at different moments of time for $k = 0.5$, i.e, for transition from the steady state regime with $K = K_1 = 0.0906$ to the regime corresponding to $K = K_3 = 0.1070$ (the other numerical parameters are the same as in 1° of Section 3). The time step $\Delta t = 0.01$; the coordinate step $\Delta x = 0.01$; the scale of the times for which the curves are drawn is $\Delta T = 0.41$. The time for establishing the new oxidizer flowrate is $\Delta T$. The upper curve is the steady-state pressure distribution for $K = K_1$, the lower curve is for $K = K_3$.

After change of the oxidizer flowrate through the channel, a simple rarefaction wave begins to propagate and is reflected alternately from the left and right boundaries. The wave intensity is low; the temperature and concentration perturbations are transported with the gas stream.

Reflection from the boundaries takes place as from a solid wall, i.e., in phase opposition with the incident wave. As in case 1° of the present section, the rarefaction wave gradually decays and the wave front diffuses. In this case the wave also decays because of the fact that it is mechanically unstable and the distribution of the quantities in the wave becomes smoother in the course of time.

The behavior of the gas temperature at the end of the channel is interesting. After the first reflection of the rarefaction wave from the nozzle, the gas temperature decreases below the steady-state value corresponding to $K = K_1$ and then begins to slowly increase, approaching the final steady-state distribution with $K = K_3$.

Since the transient processes are associated with propagation through the channel of shock waves (or rarefaction waves), it is clear that burnup of the channel also takes place in a wavelike fashion. This is seen from Fig. 3b which shows the initial ($K = K_1$) and final ($K = K_3$) distributions of the mass burning velocity $m(x)$ (denoted by letters a and b, respectively) and also the instantaneous distributions of $m(x)$ up to the moment of wave reflection from the channel entrance for several moments of time (time scale same as in Fig. 3a). The dash-dot curves correspond to waves reflected from the nozzle. We note that for steady-state burning the maximal burnup of the fuel channel occurs at the entrance to the channel, since the behavior of the function $m(x)$ is determined by the concentration distribution (the flow changes only slightly).

In conclusion let us examine Fig. 4, which shows the pressure $p_l$ at the exit from the channel as a function of time. Curve 3 is plotted for case 1° of this section, curve 2 is for case 2°, and curve 1 is for the case $k = 1.5$ (transition from the steady regime with $K = K_1$ to the regime with $K = K_2$). The latter case is associated with the formation of a compression wave (its intensity is $\Delta p/p_1 = 1/20$).

The abscissa scale in Fig. 4 is: point 100 corresponds to the time $t = 41$ for curves 1 and 2 and to $t = 30.75$ for curve 3.

The magnitude of the pressure at the channel exit changes abruptly when the shock wave (or rarefaction wave) reaches the nozzle. Since the wave decays, the magnitude of these shocks diminishes in the course of time and at the end of the process there is a smooth transition to the final steady-state value.

In Fig. 4 the lower dashed line is the final steady value for curve 2, the middle line is for curve 3, the upper line is for curve 1. Extrapolating curves 1, 2, 3 to their intersection with the corresponding straight lines, we obtain the exact times for transition to the new steady-state regime. For curves 1 and 2 $t_1 = 57.40$, for curve 3 $t_1 = 31.36$. This result differs considerably from the estimates of the emptying (or filling) time calculated from the steady-state distributions. The pressure pulsation decay time is about one third of the time for transition to the new steady regime for curves 1 and 2 and about one half the transition time for curve 3.

The transient regime computational scheme proposed in the present study is based on the assumption of the diffusive combustion mechanism for the combustion of the solid propellant, which is satisfied if there is excess oxidizer in the channel and the Reynolds number, which determines the burning velocity, is sufficiently small. Characteristic of this case is the fact that the burning velocity does not depend explicitly on the pressure.

With increase of the Reynolds number, accompanied by intensification of the burning process, there is more intense mixing of the gas at each section of the channel and a change from the diffusion combustion regime to the kinetic regime, in which the characteristic chemical reaction time is comparable with the mixing time. In this case the burning velocity depends on the pressure in accordance with the chemical reaction kinetics and the combustion regime itself in the channel is quite similar to combustion in a homogeneous chemical reactor. It is not impossible that the existence of the explicit dependence of the burning velocity on the pressure may lead to the onset of thermokinetic oscillations in the channel because of feedback between the burning velocity and the gas discharge through the nozzle, which also depends on the pressure.

Additional effects may arise in examining the restructuring of the thermal layer in the solid matter, which leads to change with time of the effective heat of combustion of the fuel. Account for the unsteady nature of the thermal layer in the transient regime is also essential in the case of diffusive combustion, provided the fuel channel emptying time is comparable with the time for restructing of the thermal layer. This effect is not considered in the present study in order to simplify the calculations. In order that the

assumption of quasistationarity of the thermal layer be justified in practice, the volume of the fuel channel must be sufficiently large – in this case the heated layer will be able to follow the state of the gas flow in the channel.

Also of interest is the solution of the transient regime problem when the oxidizer supply to the channel is deficient. In this case the oxidizer burns up completely at some channel length and in the remainder of the channel there will be ablation of the fuel under the influence of the hot combustion products rather than combustion.

In conclusion, we note that the system of equations (2.3) can be solved by averaging all the equations with regard to x. In this case the solution does not account for the gasdynamic picture of the phenomenon, which has a significant effect on the average characteristics of the transient regime. Specificially, the values of the time for transition from one steady regime to another obtained using this approach differ considerably from the actual values obtained by numerical integration of the unsteady system of equations.

The authors wish to thank L. A. Chudov for valuable advice.

## LITERATURE CITED

1. Ya. B. Zel'dovich, "On the theory of the burning of solid propellants and explosive substances," ZhETF, Vol. 12, Nos. 11, 12 (1942).
2. Ya. B. Zel'dovich, "On the stability of solid propellant burning in a semiclosed space," PMTF, Vol. 4, No. 1 (1963).
3. Ya. B. Zel'dovich, "On the burning velocity of a solid propellant at variable pressure," PMTF, Vol. 5, No. 3 (1964).
4. B. V. Novozhilov, "Transient processes in solid propellant combustion," PMTF, Vol. 3, No. 5 (1962).
5. A. G. Istratov, V. B. Librovich, and B. V. Novozhilov, "An approximate method in unsteady burning velocity theory," PMTF, Vol. 5, No. 3 (1964).
6. B. V. Novozhilov, "Average burning rate of a powder with harmonically varying pressure," Fizika goreniya i vzryva [Combustion, Explosion, and Shock Waves], No. 3 (1965).
7. O. I. Leipunskii, V. I. Kolesnikov-Svinarev, and V. N. Marshakov, "Unsteady burning velocity of a solid propellant," Dokl. AN SSSR, Vol. 154, No. 4 (1964).
8. M. Barrere, A. Jaumotte, B. Fraeijs de Veubeke, and J. Vandenkerchove, Rocket Propulsion [Russian translation], Oborongiz, Moscow (1962).
9. G. Marxman and M. Gilbert, "Turbulent boundary layer combustion in the hybrid rocket," IX Sympos. (Internat.) on Combustion, Acad. Press, New York – London (1963).
10. V. B. Librovich, "On the ignition of solid fuels," PMTF [Journal of applied Mechanics and Technical Physics], Vol. 9, No. 2 (1968).
11. E. L. Rubin and S. Z. Burstein, "Difference methods for the inviscid and viscous equations of a compressible gas," J. Comput. Phys., Vol. 2, No. 2 (1967).